Investigation of numerical wave channel concerning absorbing boundary

R. S. Shih[1], C. R. Chou[2] & W. Y. Han[3]
[1]*Department of Civil Engineering, Tung Nan Institute of Technology, Taiwan.*
[2]*Department of Harbor and River Engineering, National Taiwan Ocean University, Taiwan.*
[3]*Fisheries Administration, Council of Agriculture, Taiwan.*

Abstract

Dissipating technics such as sponges, absorbing beaches had become an interesting technique for the simulations of numerical wave tank, recently. The simulation of a two dimensional wave tank considering absorbing boundary are investigated in this study by means of boundary element method. With the time histories of water elevation measured by a pseudo wave gage, the absorption coefficient μ_0 was verified by studying the case of solitary wave propagating over the water tank with a sponge zone fixed behind, where the sponge zone was divided into a smoothly varied μ area and a constant μ area. The purpose is to adopt an optimum combination of absorption coefficient and sponge length to minimize the reflection. Our results show that the attenuation rate of wave energy reaches 99.8% and upward, which approaches nearly 100% wave energy absorbed.

1 Introduction

Numerical wave absorption zone has been developed widely in models to decrease the influence of reflected wave. As a result of the advancement of computer technology nowadays, numerical models are widely developed, some wave channel is assumed infinitely long, or that the absorption of wave energy is complete. It is well known, however, that a numerical model should be a limited domain, numerous researches exhibit that the reflection of waves can be reduced

by fixing an open boundary behind the domain. The conception of the absorbing beach was first suggested by LeMehaute [1], which was successfully developed by Larsen and Dancy [2], Brorsen and Larsen [3] in their numerical scheme for arbitrary waves simulations. Ohyama and Nadaoka [4] developed a numerical wave absorption filter for open boundary condition in the analysis of nonlinear and irregular wave evolution, the filter is composed of a simulated sponge layer and sommerfeld's radiation condition at the outer edge of the layer, which was anteriorly suggested by Ijima *et al.* [5] and Chou [6] in their investigations on permeable coastal structures. Based on the Summerfeld's condition, Grilli et al. [7][8] developed an implict iterative radiation condition for the calculation of shoaling and breaking of periodic waves and solitary wave over gentle slopes. Karambas and Koutitas [9] simulated wave deformation in the surf zone by introducing a dispersion term due to breaking to simulate Reynolds stress which is approximated by propagating bore, and their model was extensively tested against experimental data. In this article, a sponge zone was fixed at the end of the numerical wave flume, which is composed of a smoothly varied μ area and a constant μ area with a closed boundary condition at the end, it is recommended that the absorption coefficient take a value of μ_0=0.5 and a sponge of 15~25 times the length of the water depth.

2 The numerical model

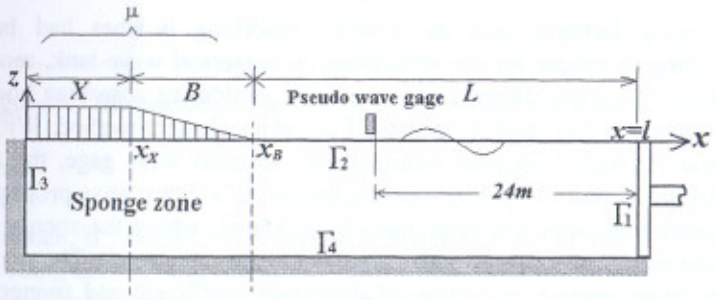

Figure 1: Definition sketch of the numerical flume.

The two-dimensional BEM was used to simulate the deformation of solitary wave by substituting a fully nonlinear boundary condition on the free water surface. As shown in Figure 1, the numerical wave tank are defined by the undisturbed free water surface; impermeable seawall; impermeable seabed and a moving wavemaker paddle, the flow within the region was assumed to be inviscid, incompressible and irrotational, boundaries are discretized using linear elements. The continuity equation is solved using the linear boundary element method based on the Green's second identity, where the velocity potential satisfies the following Laplace equation:

$$\frac{\partial^2 \Phi}{\partial x^2} + \frac{\partial^2 \Phi}{\partial z^2} = 0 \tag{1}$$

2.1 Boundary conditions

Boundary condition on the undisturbed free water surface can be obtained from the nonlinear kinematic and dynamic conditions as:

$$u = \frac{Dx}{Dt} = \frac{\partial \Phi}{\partial x} \tag{2}$$

$$w = \frac{Dz}{Dt} = \frac{\partial \Phi}{\partial z} \tag{3}$$

$$\frac{D\Phi}{Dt} + g\zeta - \frac{1}{2}\left[\left(\frac{\partial \Phi}{\partial x}\right)^2 + \left(\frac{\partial \Phi}{\partial z}\right)^2\right] + \frac{P}{\rho} = 0 \tag{4}$$

with D the Lagrange differentiation, g the gravitational acceleration, ζ the surface elevation, ρ the fluid density and P the atmospheric pressure. On the non-absorbing area, the atmospheric pressure is assumed to be constant, i.e. P=0. Along the left part of the model, referred to as sponge zone, P was suggested by Cao *et al.* [10] as:

$$P(x,\zeta) = \mu(x)\frac{\partial \Phi}{\partial n}(\zeta(x)) \tag{5}$$

$$\mu(x) = \mu_0 \rho \sqrt{gh}\left(\frac{x - x_l}{l}\right)^{\alpha} \tag{6}$$

where μ_0 is a non-dimensional absorption coefficient calculated as a function of time, x_l is the position of the beginning of absorbing beach with a length of l, and α=2~3.

In the present cases, however, the value of P was defined proportional to the free surface potential as in most earlier approaches suggested, thus, $P(x,\zeta)$ is defined as:

$$P(x,\zeta) = \mu(x)\Phi(\xi,\eta,t) \tag{7}$$

$$\mu(x) = \mu_0 \rho\left(\frac{x_B - x}{B}\right)^{\alpha} \quad , \quad x_X < x < x_B \tag{8}$$

$$\mu(x) = \mu_0 \rho \quad , \quad x \le x_X \tag{9}$$

where x_X and x_B are the horizontal coordinates of the beginning of constant μ area and smoothly varied μ area with the length of X and B, respectively. The absorption parameter of linear kind is adopted in this paper, i.e. α=1. (as shown in Figure 1)

The water particle velocity is null in the normal direction on the impermeable seawall and seabed, therefore the condition is prescribed as:

$$\frac{\partial \Phi}{\partial n} = 0 \qquad \text{on } \Gamma_3 \text{ and } \Gamma_4 \tag{10}$$

which n is the unit normal vector.

Waves can be generated by a pseudo wavemaker, though any desire type of paddle can be simulated, a piston type is adopted in this study. In this case, the boundary condition can be obtained requiring that the horizontal velocities of the wave-paddle and the fluid flow be continuous, defined as:

$$\overline{\Phi} = \frac{\partial \Phi}{\partial n} = -U(t) \tag{11}$$

For solitary wave, according to Boussinesq equation, $U(t)$ can be expressed as:

$$U(t) = \zeta_0 \sqrt{\frac{g}{h}} \cdot sec\, h^2 \left[\sqrt{\frac{3\zeta_0}{4h^3}} C(t - t_c) \right] \tag{12}$$

where ζ_0, h, C and t_c are the incident wave height, water depth, wave celerity and specific time of the semistroke of the paddle, respectively.

2.2 Governing equations and boundary discretization

The governing equations and numerical methods are briefly reviewed in the following, details can be referred to Chou and Shih [11]. According to Green's second identity, the velocity potential $\Phi(x,z;t)$ for inviscid irrotational flow can be obtained by the velocity potential on the boundary, $\Phi(\xi,\eta;t)$, and its normal derivative, $\partial\Phi(\xi,\eta;t)/\partial n$, thus

$$c\Phi(x,z;t) = \frac{1}{2\pi}\int_\Gamma \left[\frac{\partial \Phi(\xi,\eta;t)}{\partial n} \ln\frac{1}{r} - \Phi(\xi,\eta;t)\frac{\partial}{\partial n}\ln\frac{1}{r} \right] ds \tag{13}$$

$$c = \begin{cases} 1 & \textit{inside the fluid domain} \\ 1/2 & \textit{on the smooth boundary} \\ 0 & \textit{outside the fluid domain} \end{cases}$$

with $r = \left[(\xi - x)^2 + (\eta - z)^2 \right]^{1/2}$.

As shown in Figure 1, the boundaries Γ_1 through Γ_4 are devided into N_1 to N_4 discrete segments with linear elements in order to proceed with the calculations, when the inner point $(x,z;t)$ approaches the boundary point $(\xi',\eta';t)$, eqn(13) can be written in a discretized form as:

$$\begin{aligned} \Phi_i(\xi',\eta';t) &= \frac{1}{\pi}\sum_{j=1}^{N} \int_{\Gamma_j} \left[\Phi_j(\xi,\eta;t)M_1 + \Phi_{j+1}(\xi,\eta;t)M_2 \right] \frac{\partial}{\partial n} ln\frac{1}{r} ds \\ &= \frac{1}{\pi}\sum_{j=1}^{N} \int_{j} \left[\frac{\partial \Phi_j}{\partial n}(\xi,\eta;t)M_1 + \frac{\partial \Phi_{j+1}}{\partial n}(\xi,\eta;t)M_2 \right] ln\frac{1}{r} ds \end{aligned} \tag{14}$$

with $M_1 = (1-\chi)/2$, $M_1 = (1+\chi)/2$; M_1 and M_2 are the shape function within χ is a local dimensional coordinate. Hence, eqn(14) is expressed in a matrix form:

$$[\Phi_i] = [O_{ij}][\overline{\Phi_i}] \qquad i,j = 1 \sim 4 \tag{15}$$

where [Φ] and[$\overline{\Phi}$] are the nodal values of the potential function and its normal derivative on the boundaries, respectively, and [O] is a matrix related to the geometrical shape of the boundary. The numerical scheme has been discussed in detail by Chou [6].

2.3 Computational procedure

The initial conditions on each boundaries are summarized as follows: Requiring that the horizontal velocity of the pseudo wave paddle $U(t)$ and the fluid motion be continue, we obtain $\overline{\Phi}_1^0 = \partial\Phi_1^0/\partial n = -U(0)$; Assume that the water surface is initially at rest, therefore the velocity potential $\Phi_2^0 = 0$; Along the impermeable seawall and stationary bottom, no flow exist on the normal direction, i.e. $\overline{\Phi}_3^0 = \partial\Phi_3^0/\partial n = 0$.

Substituting the initial boundary conditions into eqn(15), initial values for the normal derivative of velocity potential on the water surface, $\partial\Phi_2^0/\partial n$, the velocity potentials on the pseudo wave paddle, Φ_1^0, as well as the velocity potentials on the sea wall and seabed, Φ_3^0 and Φ_4^0, can be obtained, respectively. With eqns(2)~(4), the new position for each nodal point on the water surface at k+1-th time step (k=0,1,2,3....) can be calculated using the forward difference method, thus, the velocity potential of the free water surface at the k+1-th time step Φ_2^{k+1} can be approximated through the following equation:

$$\Phi_2^{k+1} = \Phi_2^k + \frac{1}{2}\left[\left(\frac{\partial \Phi_2}{\partial s} \right)^2 + \left(\frac{\partial \Phi_2}{\partial n} \right)^2 \right]^k \Delta t - g z^{k+1} \Delta t - \frac{P^k}{\rho} \Delta t \tag{16}$$

where s is the tangential derivative, Δt denotes the discrete time differencing interval. By substituting the calculated value for the k+1-th time step and eqn(16)

to eqn(15), we obtain the following simultaneous equations:

$$\begin{bmatrix} \Phi_1 \\ \overline{\Phi}_2 \\ \Phi_3 \\ \Phi_4 \end{bmatrix}^{k+1} = \begin{bmatrix} I & -O_{12} & 0 & 0 \\ 0 & -O_{22} & 0 & 0 \\ 0 & -O_{32} & I & 0 \\ 0 & -O_{42} & 0 & I \end{bmatrix}^{-1} \begin{bmatrix} O_{11} & 0 & O_{13} & O_{14} \\ O_{21} & -I & O_{23} & O_{24} \\ O_{31} & 0 & O_{33} & O_{34} \\ O_{41} & 0 & O_{43} & O_{44} \end{bmatrix} \begin{bmatrix} \overline{\Phi}_1 \\ \Phi_2 \\ \overline{\Phi}_3 \\ \overline{\Phi}_4 \end{bmatrix}^{k+1} \tag{17}$$

I is a unit matrix. The iterative scheme of time stepping are referred in detail by Chou and Shih [11].

3 Applications

In this study, initial wave of heights ζ_0/h=0.05、0.1、0.2 and 0.3 are generated in a 30m long numerical wave channel with a constant depth of h=1m, a sponge zone is fixed behind, where the sponge zone is divided into a smoothly varied μ area and a constant μ area, the lengths of which are expressed as B and X respectively. To explore an optimum combination of absorption coefficient and sponge length to minimize the reflection, length of X =5m, 10m, 15m and B =5m, 10m, 15m are used in the simulation with μ_0=0~0.5, where the time derivation is adopted as $\Delta t=t_c/200$. Figure 2 shows time histories of the incident and reflective wave for the case with X=10m, B=15m and ζ_0/h=0.05, simultaneously. To investigate over the absorption rate in terms of the combination of various B, X and μ_0, a pseudo wave gage is placed at the position of x=24m for the measurement of water elevation, as shown in Figure 1. The total energy for solitary wave was expressed as:

$$E = \frac{8}{3}\rho g h \zeta \sqrt{\frac{\zeta}{3h}} \tag{18}$$

$$K_L = (1 - \frac{E_R}{E_I}) \times 100\ \% \tag{19}$$

where K_L is the attenuation rate, E_I and E_R are the total energy of incident and reflected wave, respectively.

4 Results and Discussions

4.1 Variation of surface elevation

As previously indicated, the measurement of water elevations was carried out by a pseudo wave gage, hence, the reflective wave height of case with ζ_0/h=0.05, X=10m and B=5m is ζ/h=0.05 when μ_0=0.0, which means the wave is completely reflected, else, the reflected wave heights for μ_0=0.1, 0.2, 0.3 are ζ/h=0.032, 0.021, 0.014, respectively, and decrease to 0.006 when μ_0=0.5. Alter the length

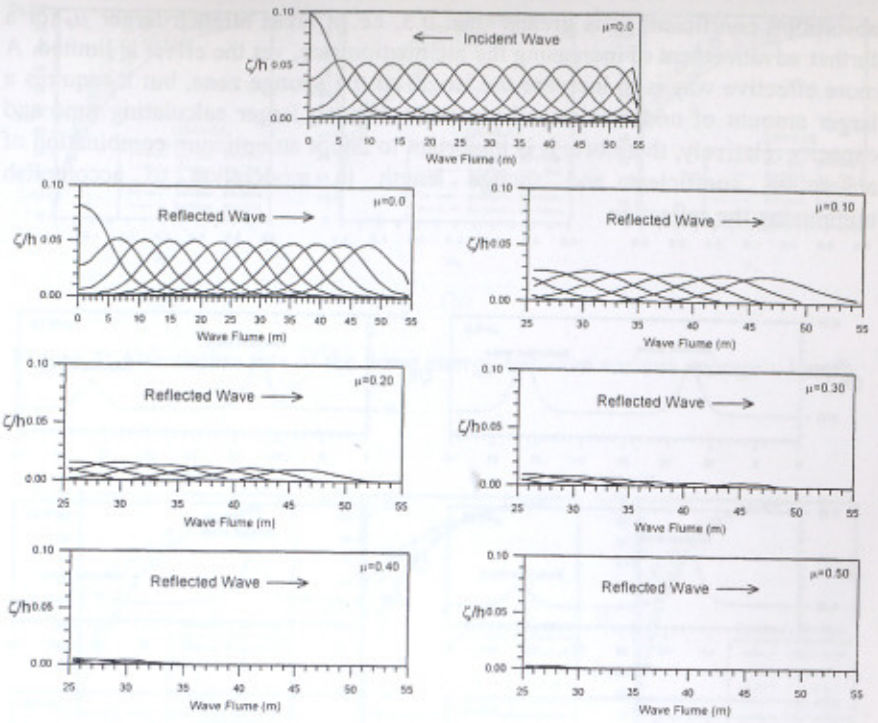

Figure 2: Time histories of the incident and reflective wave for the case with X=10m, B=15m and ζ_0/h=0.05.

of the sponge zone to various combinations of B and X, Figure 3 shows the variations of surface elevations with the condition of ζ_0/h=0.05, B=15m, X=10m and μ_0=0~0.5, the left parts of the figures showed the elevations of initial wave which revealed identically, while the right parts showed the reflected wave simultaneously, as shown in the figure, the reflected wave height decrease gradually, that the reflected wave heights for μ_0=0.1, 0.2, 0.3 are ζ/h=0.027, 0.015, 0.008, respectively, and decrease to 0.00087 when μ_0=0.05, which shows approximately null, thus it can be seen that the combination of B=15m acquire a better result than B=5m.

4.2 Attenuation rate of wave energy

The attenuation rate of case with solitary wave are calculated using Eqn(19), as shown in Figure 4(a)~(c), the length changing of the smoothly varied μ area has apparently raised the absorption efficiency. Take Figure 4(a) for example, the attenuation rate of the wave energy is 93.2% at B=10m, X=5m and μ_0=0.5, and increases up to 99.9% when B=10m, X=15m and μ_0=0.5, which indicates approximately complete dissipated. The curvature grows gently when the

absorption coefficient μ_0 is greater than 0.5, i.e. it takes a much larger μ_0 for a further advancement of increasing the attenuation rate, yet the effect is limited. A more effective way is to increase the length of the sponge zone, but it requires a larger amount of nodal points which cause a much larger calculating time and capacity relatively, therefore, it is important to adopt an optimum combination of absorption coefficient and sponge length in moderation to accomplish minimizing the reflection.

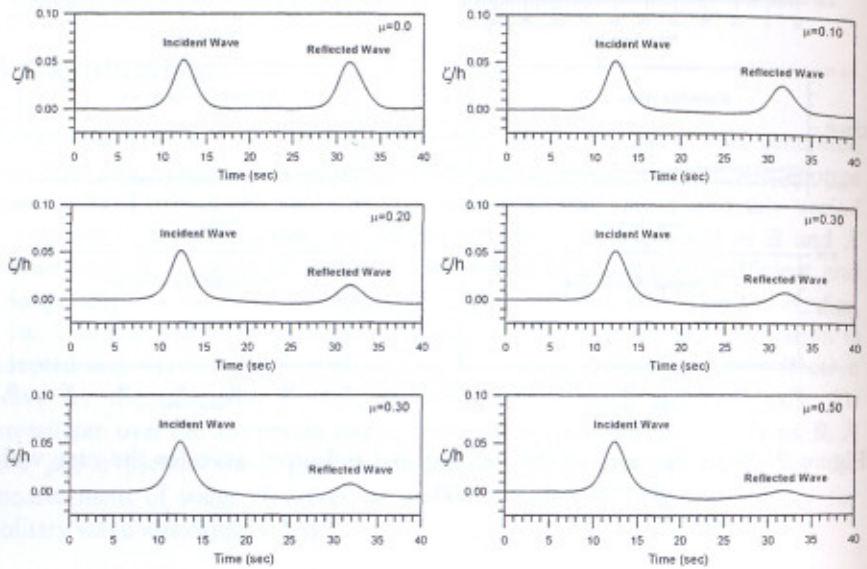

Figure 3: Variation of surface elevations with the condition of X=10m, B=15m, ζ_0/h=0.05 and μ_0=0−0. 5.

Besides, comparing Figure 5(a)~(c) simultaneously, though the attenuation rate increase up to 50% when μ_0=0.1, it obtained unfavorable results for μ_0=0 as the incident wave height raise up gradually, it may due to the insufficiency of the amount of elements. Figure 5(a)~(c) exhibits the curve of attenuation rate regarding dissipation coefficient μ_0 for different wave heights, which the absorption increases quite substantially for waves of small heights when μ_0<0.3, furthermore, the absorptions tend to become identical after $\mu_0 \geq$ 0.3, that is to say, the attenuation rate approached closely to the same value in terms of waves with arbitrarily heights when $\mu_0 \geq$ 0.3.

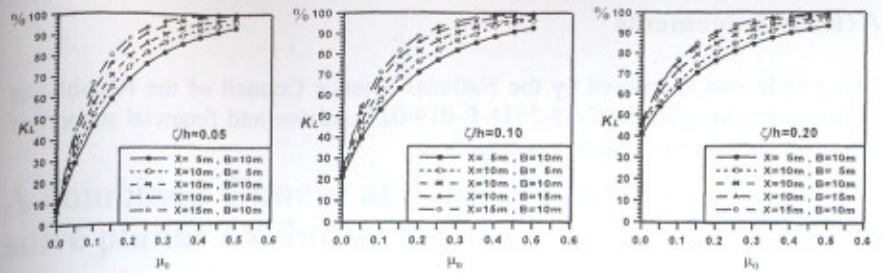

Figure 4: Attenuation rate of the wave energy between various sponge's length.

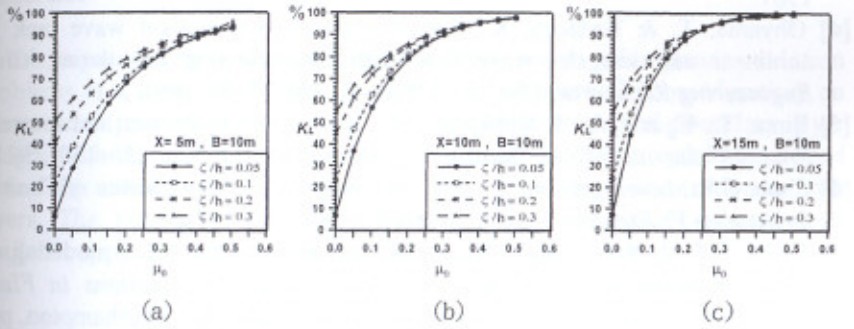

Figure 5: Attenuation rate of the wave energy between various wave heights.

5 Conclusion

The generation of solitary waves and the use of absorbing boundary are illustrasted in this research in which showed good absorptance. The attenuation rate increases not only because of the enlargement of the μ_0's value but also the length of the sponge zone, nevertheless, both process exist some defects. A optimum combination of absorption coefficient μ_0, X and B we found presently is taken as μ_0=0.5, X=15m and B=10m, which raised the attenuation rate of the wave energy up to 99.8%, this result signifies that the wave energy is approximately complete dissipated, and indicates favorable agreement. The numerical scheme should be apply to the modeling of periodical and irregular waves in our further extension.

Acknowledgements

This article was sponsored by the National Science Council of the Republic of China under the grant NSC-89-2611-E-019-027. Advice and financial support of the council are gratefully acknowledged.

References

[1] LeMehaute. B., Progressive wave absorber. *J. Hyd. Res.*, **10(2)**, pp. 153–169, 1972.

[2] Larsen, J. & Dancy, H., Open boundaries in short wave simulations—A new approach. *Coastal Engineering*, **7**, pp. 285–297, 1987.

[3] Brorsen, M. & Larsen, J., Source generation of nonlinear gravity waves with the boundary integral equation method. *Coastal Engineering*, **11**, pp. 93–113, 1987.

[4] Ohyama, T. & Nadaoka, K., Development of a numerical wave tank in nonlinear and irregular wave field with non-reflecting boundaries. *Civil Engineering Rechearch*, J.S.C.E., **429(II-15)**, pp. 77–86, 1991.

[5] Ijima, T., Eguchi, Y. & Kobayashi, A., Permeable breakwater and seawall. *Proc. 18st Japanese Conf. Coastal Engineering*, J.S.C.E., pp. 121–130, 1971.

[6] Chou, C.R., *Investigations of wave deformation with the influence of Coastal Structures*, Ph.D. thesis, Kyushu University: Kyushu, 1976.

[7] Grilli, S.T. & Subramanya, R., Recent advances in the BEM modeling of nonlinear water waves (Chapter 4). *Topics in BE Applications in Fluid Mechanics*, ed. H. Power, Wessex Institute of Technology: Southampton, pp. 91–122, 1995.

[8] Grilli, S.T., Svendsen, I.A. & Subramanya, R., Breaking criterion and characteristics for solitary waves on slopes. *Journal of Waterway, Port, Coastal and Ocean Engineering*, **123(3)**, pp. 102–112, 1997.

[9] Karambas, Th.V. & Koutitas. C., A breaking wave propagation model based on the Boussinesq equation. *Coastal Engineering*, **18**, pp. 1–19, 1992.

[10] Cao, Y., Beck, R.F. & Schultz, W.W., An absorbing beach for numerical simulations of nonlinear waves in a wave tank. *Proc. 8st Int. Workshop WaterWaves and Floating Bodies*, St. John's: Newfoundland, pp. 17–20, 1993.

[11] Chou, C.R. & Shih, R.S., Generation and deformation of solitary waves. *China Ocean Engineering*, **10(4)**, pp. 419–432, 1996.